*Desalination and Water Treatment*
www.deswater.com
doi: 10.5004/dwt.2023.30010

313 (2023) 57–65
November

# Study of the treatment efficiency of cuttlefish conditioning effluent using low-cost zeolite/sand composite microfiltration membrane

Hajer Aloulou[a,b], Wala Aloulou[a], Raja Ben Amar[a,*]

[a]*Research Unit 'Advanced Technologies for Environment and Smart Cities', UR22ES02, emails: benamar.raja@yahoo.com (R. Ben Amar), hajer.aloulou89@yahoo.fr (H. Aloulou), walaaloulou6@gmail.com (W. Aloulou)*
[b]*Department of chemical, Preparatory Institute for Engineering Studies of Gabes, Gabes 6029, Tunisia*

Received 21 June 2023; Accepted 20 September 2023

**ABSTRACT**

In this work, zeolite/sand microfiltration membrane prepared by deposition of a thin layer on a tubular support (active layer/support) was applied for the purification of industrial wastewater. The results were compared to that made by zeolite/zeolite and sand/sand microfiltration membranes. The effect of the membrane support was determined by the estimation of the membrane fouling established during the filtration. Therefore, permeate flux, fouling resistances and treatment efficiencies were thoroughly compared. The utilization of zeolite membrane over sand support (zeolite/sand) instead of the membrane totally on zeolite (zeolite/zeolite) shows an increase in the stabilized permeate flux from 58 to 180 L/h·m$^2$ at 1 bar. Whereas, the membrane totally made from sand (sand/sand) displayed a higher stabilized permeate flux of 464 L/h·m$^2$. For zeolite membrane, the increase of the flux recovery ratio from 44.94% to 54.62% and the decrease of flux decay ratio from 89.13% to 83.3%, using sand support instead of zeolite, indicate better antifouling properties. The maximum chemical oxygen demand (COD) rejection of 97% was achieved using sand/sand membrane. For zeolite membranes, an increase in COD rejection from 57% to 73% was obtained when the sand support was used instead of zeolite. Overall, the uses of sand support for the zeolite membrane enhanced permeate flux, antifouling properties and separation efficiencies. Therefore, the sand material appears suitable as support for composite membrane elaboration.

*Keywords:* Microfiltration; Natural sand; Natural zeolite; Treatment performances; Membrane fouling

## 1. Introduction

It is well known that water is an essential resource on the earth for any living things [1,2]. The economic development and the rapid industrialization lead to the increase of wastewater volumes released into the environment which pose serious problems of contamination [3,4]. As the potable water resources are limited, the treatment of industrial effluents is required to reduce the pollution [5]. In addition, the reuse of treated water in industrial activities can solve partially the water crisis. Among the different methods for wastewater treatment, membrane separation is usually used because of its performances and dependability for continuous processing [6]. This technology was applied mainly in the sectors of biotechnology, pharmacy, chemistry, in agri-food industry and water purification [7–15].

Microfiltration (MF) is a promising membrane separation technology that was largely adopted for many industrial applications such as wastewater treatment, protein separation, juice clarification, bacteria separation and several environmental applications [16–18]. In addition, MF technology is an emerging alternative for classical separation treatments offering easy separation performance, good selectivity, continuous and automatic operation [19]. The major advantages of MF membranes are related to their uniform pore sizes and low energy needed for the functioning due

* Corresponding author.

to low pressures used [20,21]. Nowadays, the fabrication of MF membranes from inorganic materials has attracted attention in wastewater purification because of their excellent thermal stability, chemical resistance and mechanical strength, offering long-life performance and minimal pollution impact in comparison with polymer membranes [22].

In general, the fabrication of inorganic membranes is characterized by high material cost and rough preparation conditions that requires several steps such as grinding, sieving, preparation of a plastic paste, extrusion and consolidation by sintering. Therefore, researchers were pushed to develop low-cost ceramic membranes using natural materials such as clay [23,24], zeolite [25,26], sand [27], phosphate [28,29], bentonite [30]. Low-cost membranes can be prepared also from coproduct coming from industries transformation such as mud [31] and fly ash [32,33]. Several researches, in the domain of wastewater treatment, have proven the high performance of natural inorganic materials during microfiltration process. Mouiya et al. [34] developed flat membrane made from clay and phosphate for the purification of industrial wastewater and water desalination. High turbidity removal more than 99% was achieved. Bouazizi et al. [30] developed a Moroccan bentonite microfiltration membrane for the treatment of tannery and textile effluents. They found that the tested membranes allow a good retention of suspended particles between 94% and 99%. Aloulou et al. [35] observed oil removal of 99.1% after treatment of industrial oily wastewater by a zeolite MF membrane at 1 bar and 60°C. While, Beqqour et al. [36] used micronized phosphate and natural pozzolan for the fabrication of MF membrane, applied to the clarification of industrial wastewaters. 97.83% and 99.77% of turbidity removal was observed, respectively for tannery wastewater and aluminium chloride suspension. Overall, these studies show that ceramic MF membrane can significantly reduce the pollutants from wastewaters. However, inevitable membrane fouling issues are still limited the use of membrane technology due to the limitation of the permeate flux as well as membrane lifetime [37,38]. Therefore, membrane fouling is an urgent problem that needs to be solved in MF treatment. In order to improve the efficiency of the process in terms of permeate flux, a new strategy may be set in preparing low-cost membranes from natural materials over support characterized by large pore diameters to control membrane fouling.

The principal purpose of this paper is the development and the characterization of new composite MF membrane based on zeolite and sand through the determination of the performances during the purification of cuttlefish conditioning effluent. Achievable permeate flux, fouling resistances, and purification efficiencies were compared for the different MF membranes (zeolite/zeolite, sand/sand and zeolite/sand) to confirm the advantages of the new composite membrane based on zeolite as active layer over sand support.

## 2. Experimental set-up

### 2.1. Materials

A tubular sand support previously fabricated was utilized for the preparation of the new composite zeolite/sand membrane. This low-cost ceramic support (sintered at 1,250°C) presents an average pore size of 10.36 μm, high porosity of 44.72%, excellent mechanical strength of 15.14 MPa and water permeability of 3,611 L/h/m$^2$·bar [27].

The decanted zeolite powder, previously described in our work [39], was chosen as material to be deposited as active layer for the preparation of the new MF zeolite/sand membrane.

Polyvinyl alcohol (Rhodoviol 25/140) as additive and ethanol as rinsing solvent were purchased from Prolabo and Chemi-Pharma.

### 2.2. Fabrication of the composite zeolite/sand membrane

At first, the sand support was washed with hot water then with ethanol via ultrasound irradiation for 40 min to eliminate residual particles. The cleaned support was dried overnight at 100°C. In the second step, 2% of decanted zeolite powder was mixed with 68% of water and 30% of PVA (12 wt.% aqueous solution) under magnetic stirring. Then, the sand support was coated using the zeolite/PVA suspension by layer-by-layer technique [40]. Finally, the green membrane was kept in air for 1 d then sintered in a programmable furnace at 1,000°C during 3 h.

### 2.3. Membrane characterization

The membrane morphology was determined using a scanning electron microscopy (SEM) (MERLIN scanning electron microscope by ZEISS associated with a GEMINI II column, Göttingen, Germany). The preparation of our samples for SEM analyses consists of three main steps:

- Rinsing the surface with ethanol,
- Drying in an oven at 90°C for 24 h (checking the stability of the mass),
- Applying a thin layer of palladium by plasma sputtering.

The average pore size of membrane was determinate using the extended Hagen–Poisseuille equation [41]:

$$d = 2\sqrt{8 \cdot J_w \cdot \delta \cdot \frac{\tau}{\varepsilon} \cdot \frac{\Delta X}{\Delta P}} \quad (1)$$

where $d$ (m) is the pore diameter, $J_w$ (m/s) is the water flux, δ (Pa·s) is the water viscosity, τ is the tortuosity factor (2.5 for sphere particle packing), ε (%) is membrane porosity, $\Delta P$ (Pa) is the applied pressure, and $\Delta X$ (m) is the membrane thickness.

### 2.4. Microfiltration experiment

The cross-flow filtration test was conducted using a stainless steel unit described elsewhere [42]. Before the filtration test, the membrane was conditioned in distilled water for 24 h. Water permeability $L_p$ (L/h/m$^2$·bar) of the new composite membrane (zeolite/sand) was performed by the filtration of distilled water per 1 bar at room temperature. This parameter was determined using Darcy's low by studying the variations of the water permeate flux $J_w$ (L/h·m$^2$) with the transmembrane pressure $\Delta P$ (bar):

$$L_p = \frac{J_w}{\Delta P} \quad (2)$$

$$J_w = \frac{V}{S \cdot t} \quad (3)$$

where $V$ (L) is the volume of water permeate collected during 1 h (h), $S$ is the membrane area ($m^2$).

The efficiencies of three membranes zeolite/zeolite, sand/sand and zeolite/sand were evaluated by filtration of cuttlefish conditioning effluent during 1 h at ambient temperature and under a pressure of 1 bar. The normalized flux ($J_N$) was obtained by the fraction of the permeate flux at a given time $t$ ($J$) by the initial permeate flux ($J_0$).

Cuttlefish wastewater comes from the conditioning of cuttlefish by washing before freezing to eliminate black color caused by the ink contained in the animal bag which generates highly colored wastewater. As pretreatment, the effluent was filtrated by a sieve of 100 μm before MF experiment to eliminate large particles.

### 2.5. Characterization of the raw and treated wastewaters

The physicochemical parameters of the raw wastewater to be treated by zeolite/sand membrane are reported in Table 1. The application of the zeolite/zeolite and sand/sand membranes for the purification of the same type of wastewater was previously tested in our previous works [25,27].

The raw and treated wastewater was characterized by measuring the pH, conductivity, turbidity and chemical oxygen demand (COD). The turbidity was measured by a turbidity meter (model 2100A, Hach) in agreement with standard method 2130B. The COD was obtained using a colorimetric technique (COD 10119, Fisher Bioblock Scientific). The conductivity and pH were measured by a conductivimeter (EC-400L, Istek, Inc.) and a pH meter (pH-220L, Istek, Inc.).

The rejection $R$ (%) of turbidity and COD was calculated according to Eq. (4) [43,44]:

$$R_x = \frac{\left(X_{\text{feed}} - X_{\text{permeate}}\right)}{X_{\text{feed}}} \times 100 \quad (4)$$

where $X_{\text{feed}}$ and $X_{\text{permeate}}$ are the values of turbidity and COD of raw and treated wastewater, respectively.

### 2.6. Modeling of membrane fouling

Hermia model was applied to describe the decrease of the membrane flux during the clarification of the wastewater by microfiltration process. This model was based on four empirical approaches: complete pore blocking [Eq. (5)], standard pore blocking [Eq. (6)], intermediate pore blocking [Eq. (7)] and cake filtration [Eq. (8)] [45].

$$\ln\left(J_w^{-1}\right) = \ln\left(J_0^{-1}\right) + K_b t \quad (5)$$

$$J_w^{-0.5} = J_0^{-0.5} + K_s t \quad (6)$$

$$J_w^{-1} = J_0^{-1} + K_i t \quad (7)$$

$$J_w^{-2} = J_0^{-2} + K_c t \quad (8)$$

where $J_w$ is the permeate flux, $t$ is the time of filtration, $J_0$ is the $y$-intercept and $K$ is the slope.

### 2.7. Calculation of different fouling resistance abilities

The fouling resistance ability of the three membranes zeolite/zeolite, sand/sand and zeolite/sand were evaluated at 1 bar after 1 h of filtration. Two parameters namely flux recovery ratio (FRR) and flux decay ratio (FDR) could be calculated using Eqs. (9) and (10) [46]:

$$\text{FDR} = \frac{J_w - J_c}{J_w} \times 100 \quad (9)$$

$$\text{FRR} = \frac{J_{\text{wa}}}{J_w} \times 100 \quad (10)$$

where $J_w$ is the water permeate flux of the clean membrane, $J_c$ is the stabilized permeate flux of the membrane using the wastewater. $J_{\text{wa}}$ is the water permeate flux of the membrane measured after physical cleaning of the membrane with distilled water after purification of wastewater.

Table 1
Main characteristics of the raw cuttlefish conditioning wastewater

| Sample | Raw wastewater |
|---|---|
| pH | 7.82 |
| Conductivity (mS/cm) | 1.24 |
| Turbidity (NTU) | 188 |
| COD (mg/L) | 1350 |

## 3. Results and discussion

### 3.1. Characterization of the composite zeolite/sand membrane

#### 3.1.1. Membrane morphology and pore size analysis

The top surface of the zeolite/sand membranes sintered at 900°C and 1,000°C are shown in Fig. 1. It is clear from SEM micrographs (Fig. 1a and b) that all membranes surface are homogenous and without cracks.

At 900°C, intergrain pores between grains are relatively large and the consolidation of particles is weak to enough suitable ceramic body [21] (Fig. 1a). It can be seen that this membrane depicts the presence of small-sized pores which results in its higher porosity. Thus, this temperature seems inappropriate to ensure good sintering. At 1,000°C, it is clear that intergranular contact between particles is reduced and consequently large pores were created compared to the membrane sintered at 900°C (Fig. 1b). The absence of smaller pores is likely to reduce its porosity and increase its overall pore size [47].

The membrane sintered at 1,000°C showed appropriate porous structure with strong cohesion between particles. Therefore, 1,000°C can be chosen as optimal sintering

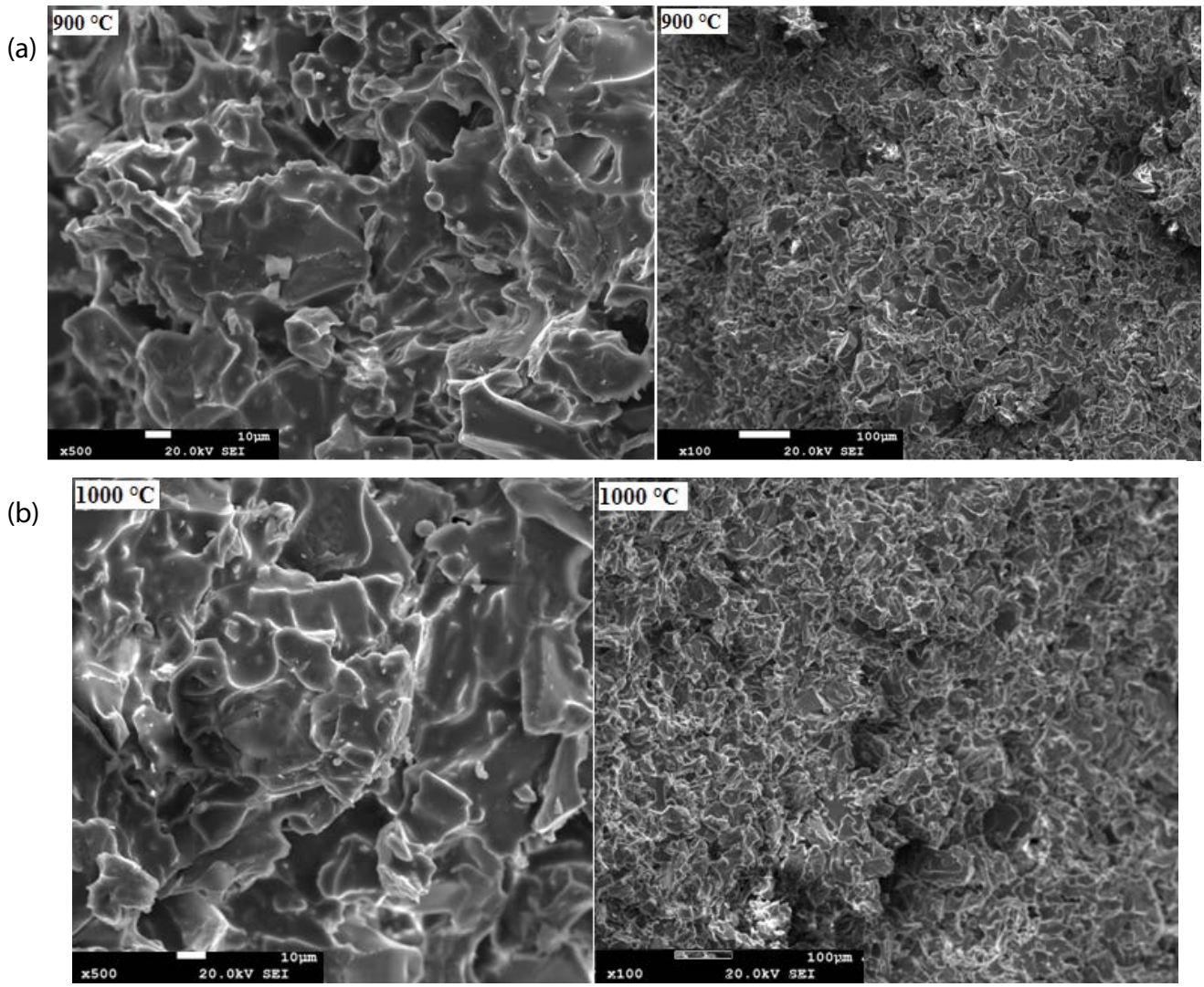


Fig. 1. Scanning electron micrographs of composite zeolite/sand membrane surface: sintered at 900°C (a) and sintered at 1,000°C (b).

temperature for zeolite/sand membrane. This retained temperature was lower than that observed with the sand/sand MF membrane obtained at sintering temperature of 1,100°C [27].

The cross-section view of the membrane sintered at 1,000°C (Fig. 2) indicated a good adhesion between the MF layer and the support which confirm the efficiency of the layer-by-layer method for the MF membrane fabrication. The thickness of the layer is about 33.3 μm which is a suitable value for preferably microfiltration layer around 10–50 μm [48].

Considering the Hagen–Poiseuille equation, the average pore size of the composite membrane zeolite/sand was estimated to be 1.2 and 1.8 μm for 900°C and 1,000°C, respectively. This result is consistent with the evolution of the average pore diameter and the porosity of the ceramic membrane with the sintering temperature which reveals that the porosity decreases while the pore diameter increases when the sintering temperature increases [49]. This behavior corresponds to an opening of the pores at low temperature. The start of the material densification occurred when the temperature increases (above 1,000°C). The pore diameter of the optimized membrane sintered at 1,000°C (1.8 μm) is larger than that of the membrane totally from sand (0.9 μm) since it is evident that the zeolite powder is finer than the sand powder consequently it cannot correctly reduce the large pores of the sand support. However, the sand particles with bigger size allow better reduction of the large pores of the sand support.

### *3.1.2. Membrane permeability*

The permeability of the membrane was determined by using deionized water. The water permeate flux of the zeolite/sand membrane was measured at different transmembrane pressures and a flux vs. transmembrane pressure curve was drawn (Fig. 3). The membrane permeability was estimated from the slope of the straight line fitted through the origin [27]. The membrane permeability value was found as 1081 L/h/m$^2$·bar. The characteristics of the different MF

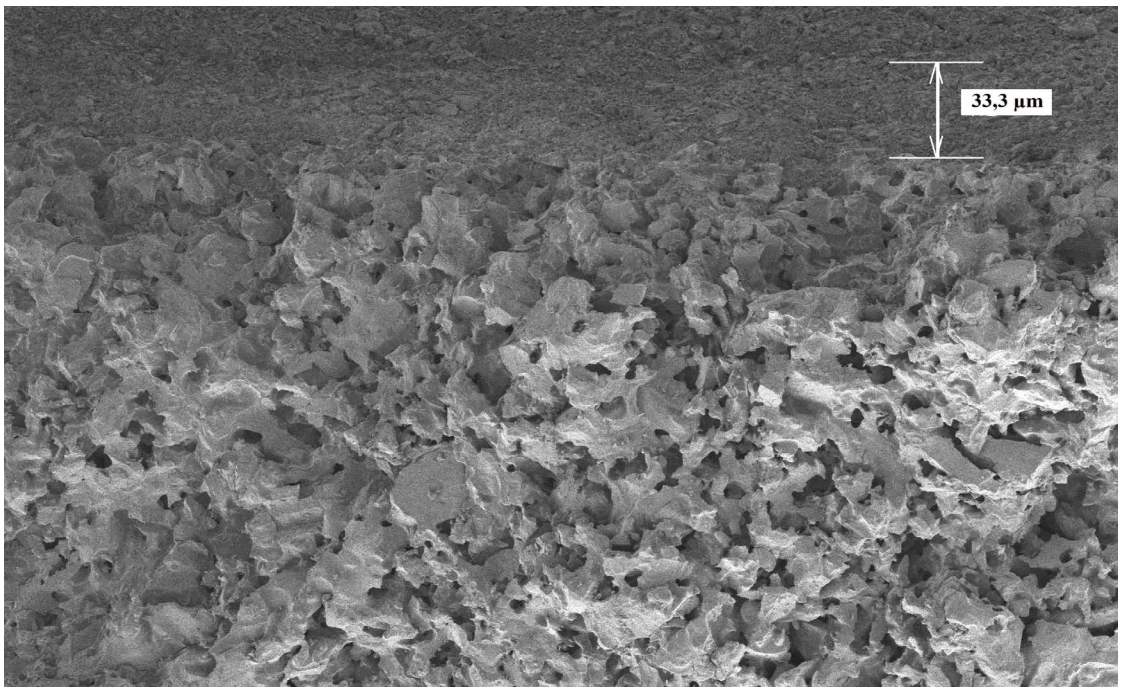


Fig. 2. Scanning electron micrograph of composite zeolite/sand membrane sintered at 1,000°C cross-section.

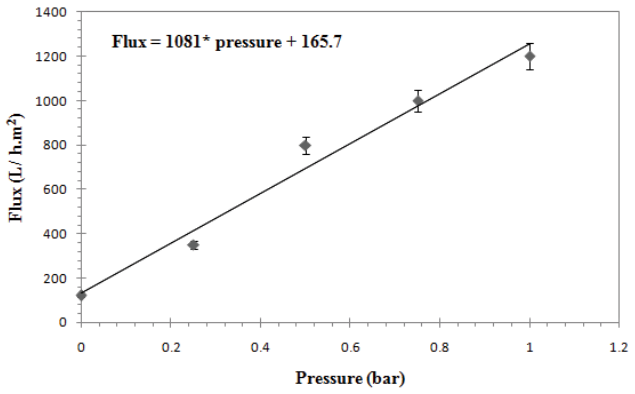


Fig. 3. Evolution of water permeate flux with pressure for zeolite/sand membrane.

membranes, zeolite/zeolite, sand/sand and zeolite/sand, are illustrated in Table 2.

### 3.2. Determination of the membranes performances

The performances of the three membranes zeolite/zeolite, sand/sand and zeolite/sand were assessed by microfiltration of cuttlefish conditioning effluent at ambient temperature and a transmembrane pressure of 1 bar. Fig. 4 presents the variation of the normalized permeate flux ($J_N$) with the filtration time. For both membranes coated on sand support (sand/sand and zeolite/sand), a rapid and significant permeate flux reduction was observed during the first 20 min. After that, stabilized normalized flux values of 0.68 for sand/sand and 0.63 for zeolite/sand were achieved after 25 min of filtration. Nevertheless, for the totally zeolite membrane (zeolite/zeolite), much lower flux reduction was observed and the normalized flux was stabilized at 0.93 after 15 min. Therefore, it appears that the fouling is more important for the membrane having the highest pore size which is in this case the zeolite/sand membrane (1.8 µm) (Table 3).

The efficiency of the purification of the three MF membranes was achieved by the determination of the removal of COD and turbidity. Fig. 5 shows that all membranes displayed encouraging abilities to eliminate the turbidity (>96%), whereas for COD removal, the values were of 97%, 73%, and 57%, respectively by sand/sand, zeolite/sand and zeolite/zeolite membranes. For the zeolite/zeolite membrane, the mass transfer is caused by the diffusion phenomena considering the low removal value of COD. However, the cake layer created by the retention of the pollutants on the MF sand/sand and zeolite/sand membranes constitutes a dynamic UF membrane superimposed on the initial MF membrane. For these membranes prepared over sand supports, having large pore sizes, the fouling of the pores occurs also which explains the higher retention of COD. Consequently, the utilization of sand support for zeolite membrane enhances the separation efficiency.

### 3.3. Fouling study

#### 3.3.1. Effect of fouling layer

Permeate flux of both sand/sand and zeolite/sand membranes sharply decreases during the first 20 min. In fact, colloidal and suspended particles contained in feed solution caused the fast clogging of the membrane pores [34]. Then, the slowly and continuously decreases of permeate flux could be caused by the slow pore clogging [21]. While, the zeolite/zeolite membrane exhibits a very slight

Table 2
Characteristics of the prepared ceramic microfiltration membranes

| Membrane | Sintering temperature (°C) | Membrane thickness (μm) | Pore sizes (μm) | Water permeability (L/h/m²·bar) | Permeate flux (at 1 bar) (L/h·m²) | Normalized flux | References |
|---|---|---|---|---|---|---|---|
| Zeolite/zeolite | 850 | 2.2 | 0.18 | 534 | 58 | 0.93 | [25] |
| Sand/sand | 1,100 | 20 | 0.9 | 1,228 | 464 | 0.68 | [27] |
| Zeolite/sand | 1,000 | 33.3 | 1.8 | 1,081 | 180 | 0.63 | This study |

Table 3
Parameters associated to various pore blocking models

| Blocking model | Zeolite/zeolite | | | Sand/sand | | | Zeolite/sand | | |
|---|---|---|---|---|---|---|---|---|---|
| | $K$ | $J_0$ | $R^2$ | $K$ | $J_0$ | $R^2$ | $K$ | $J_0$ | $R^2$ |
| Complete pore blocking | –0.003 | 4.142 | 0.879 | 0.016 | –6.521 | 0.965 | 0.007 | –5.361 | 0.926 |
| Standard pore blocking | 0 | 0.125 | 0.875 | 0 | 0.038 | 0.966 | 0 | 0.068 | 0.927 |
| Intermediate pore blocking | 0.053 | $15.86 \times 10^{-3}$ | 0.879 | 0.029 | $1.456 \times 10^{-3}$ | 0.974 | 0.04 | $4.682 \times 10^{-3}$ | 0.931 |
| Cake filtration | 1.745 | $251.7 \times 10^{-6}$ | 0.879 | 0.109 | $2.051 \times 10^{-6}$ | 0.975 | 0.415 | $21.85 \times 10^{-6}$ | 0.934 |

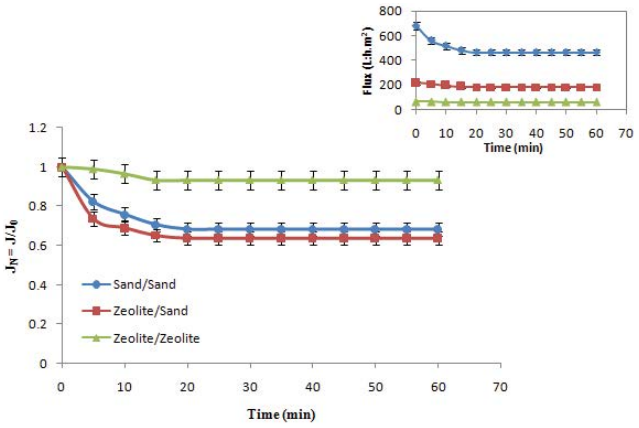


Fig. 4. Normalized flux and permeate flux vs. time using different membranes.

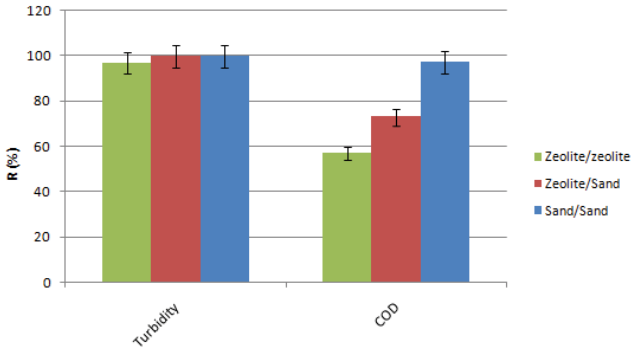


Fig. 5. Retention of turbidity and chemical oxygen demand by different membranes at 1 bar.

decrease of permeate flux. The stabilized flux of 58 L/h·m² was obtained after only 15 min of filtration. This behavior can be explained by an establishment of an instantaneously fouling layer on the membrane surface.

Fig. 6 illustrates the linearized plots of pore blocking models using the different membranes. Table 3 summarizes the associated parameters, slope, $y$-intercept and $R^2$, to the considered models. According to $R^2$ values, it appears that intermediate pore blocking and cake filtration models are able to describe the fouling for zeolite/sand and sand/sand membranes, suggesting that the wastewater contains particles equal and bigger to membranes pores (Fig. 6c and d). Indeed, the model that signifies experimental data with the best $R^2$ value (almost 1) is considered to indicate the suitable fouling mechanism during microfiltration [50]. For zeolite/zeolite membrane, $R^2$ is below 90%, therefore Hermia model does not correlate with the experimental data [51].

### 3.3.2. Membrane fouling characteristics

FRR and FDR represent the two parameters to quantify the fouling properties of the membrane. FRR associated with irreversible membrane fouling is determined by the distilled water flux before and after the effluent runs. It is worth to notice that higher FRR values are more beneficial and prove better antifouling property. The flux decline during the experimental runs was measured by FDR. Therefore, lower FDR values are more favorable [52].

Fig. 7a and b show the evaluation of the fouling coefficients FRR and FDR in the case of the three following membranes: zeolite/zeolite, sand/sand and zeolite/sand. It is clear that the sand/sand membrane presents the higher FRR value (57.8%) and the lowest FDR value (62.2%). In addition, the change of zeolite support by sand for the preparation of zeolite membrane allows the increase of the FRR from 44.94% to 54.62% and the decrease of the FDR from 89.13% to 83.3%. This result follows that related to the determination of the fouling model for each membrane. Overall, the utilization of sand support for the preparation of zeolite membrane enhanced the permeate flux, the antifouling properties and the separation efficiency.

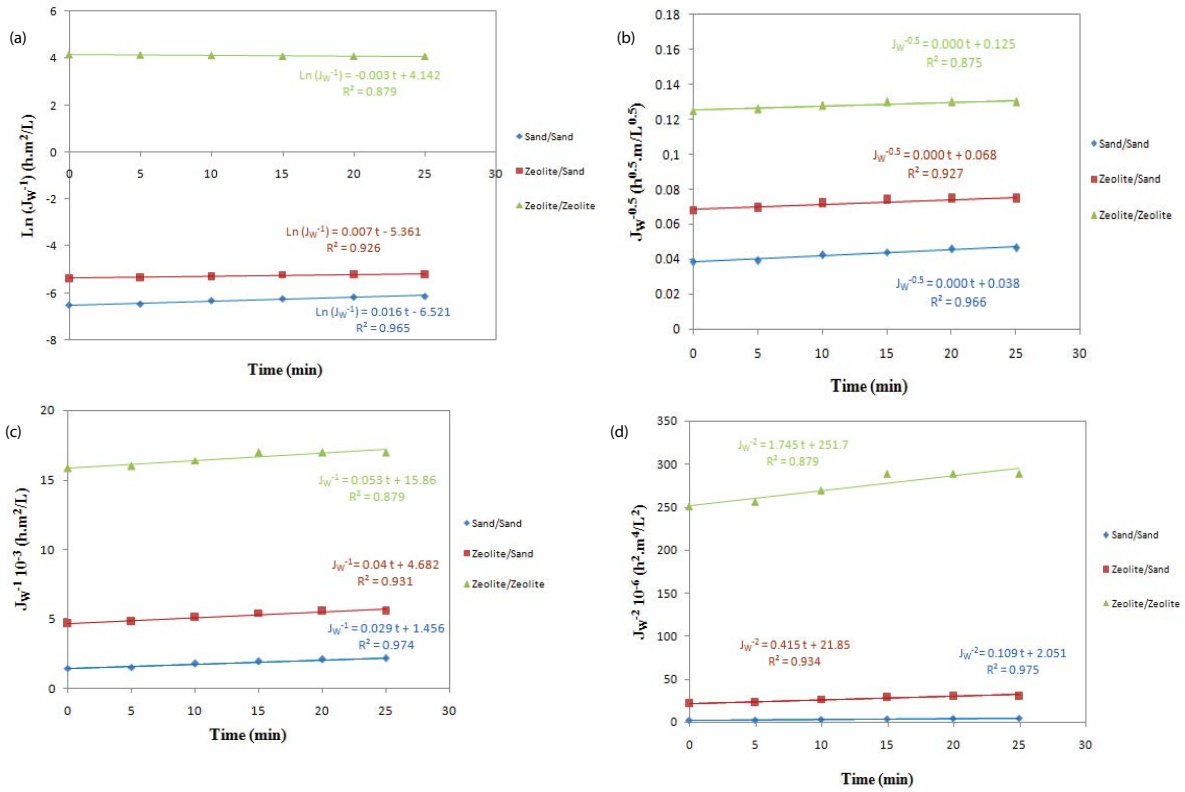


Fig. 6. Linearized models of permeate fluxes of wastewater using different membranes: complete pore blocking (a), standard pore blocking (b), intermediate pore blocking (c) and cake filtration (d).

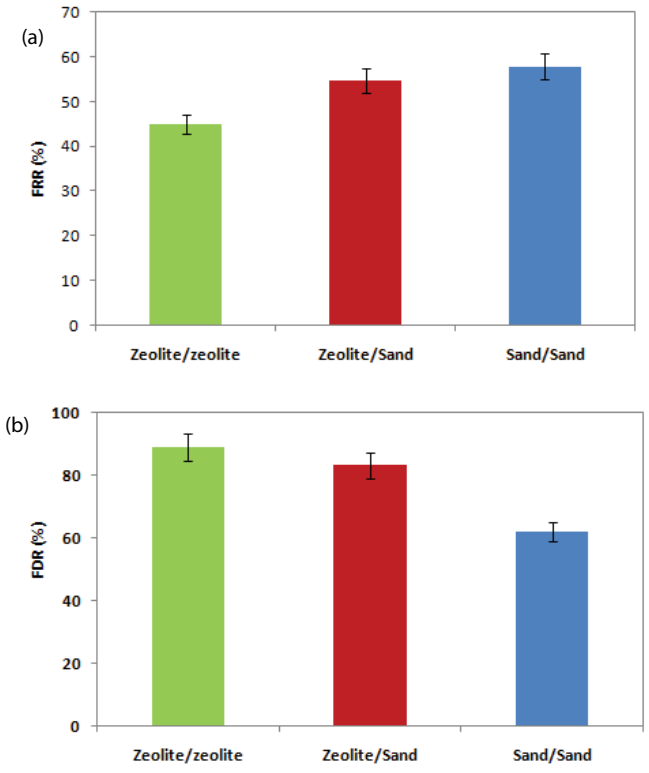


Fig. 7. Calculated flux recovery ratios (a) and flux decay ratio (b) for different membranes.

## 4. Conclusion

New composite membrane zeolite/sand was successfully prepared by coating zeolite layer over sand support via layer-by-layer method. SEM images indicated that sand/zeolite membrane have a homogeneous surface, uniform thickness (33.3 μm) and good adherence between the MF layer and the support. The pore size and water permeability were found 1.8 μm and 1081 L/h/m²·bar.

Applied to the treatment of cuttlefish effluent at ambient temperature and 1 bar, this membrane shows a good efficiency in terms of removal of turbidity (99.51%) and COD (73%) and a stabilized permeate flux of 180 L/h·m².

Relative goodness of this new composite membrane in MF process for wastewater purification was assessed by comparing its performance with two MF membranes, sand/sand and zeolite/zeolite previously prepared and tested in our laboratory. The highest flux of 464 L/h·m² was determined for sand/sand membrane while a relatively low flux of 58 L/h·m² was achieved for zeolite/zeolite membrane. In addition, the turbidity and the COD removal were in the range of 96%–99% and 57%–97%, respectively for zeolite/zeolite and sand/sand membranes. In relation to the FRR and the FDR, the application of zeolite/sand membrane for the wastewater treatment was most beneficial than in the case of membrane totally made from zeolite (zeolite/zeolite). Therefore, it can be concluded that good antifouling properties, high permeate flux and separation efficiency can be achieved with this new low-cost ceramic membrane. These finding suggest that sand support could be a promising

candidate for the preparation of composite zeolite membrane with excellent performances for the treatment of industrial effluents. Based on the encouraging results obtained in this study, optimization and scale-up studies will be carried out in the future for the treatment of wastewaters.

## Acknowledgments

The authors appreciatively acknowledge funding from PHC-UTIQUE program N° 20G1205 and TRUST Prima 2020 program (research project supported by the European commission).

## References

[1] M. Amarine, B. Lekhlif, M. Sinan, A. El Rharras, J. Echaabi, Treatment of nitrate-rich groundwater using electrocoagulation with aluminum anodes, Groundwater Sustainable Dev., 11 (2020) 1–11.
[2] N. Malik, V.K. Bulasara, S. Basu, Preparation of novel porous ceramic microfiltration membranes from fly ash, kaolin and dolomite mixtures, Ceram. Int., 46 (2020) 6889–6898.
[3] A. Azimi, A. Azari, M. Rezakazemi, M. Ansarpour, Removal of heavy metals from industrial wastewaters: a review, ChemBioEng Rev., 4 (2016) 37–59.
[4] J. Cuhorka, E. Wallace, P. Mikulášek, Removal of micropollutants from water by commercially available nanofiltration membranes, Sci. Total Environ., 720 (2020) 1–11.
[5] M.M. Damtie, Y.C. Woo, B. Kim, R.H. Hailemariam, K.D. Park, H.K. Shon, C. Park, J.S. Choi, Removal of fluoride in membrane-based water and wastewater treatment technologies: performance review, J. Environ. Manage., 251 (2019) 1–24.
[6] R.P. Lively, D.S. Sholl, From water to organics in membrane separations, Nat. Mater., 16 (2017) 276–279.
[7] R. Balti, N. Zayoud, F. Hubert, L. Beaulieu, A. Massé, Fractionation of *Arthrospira platensis* (*Spirulina*) water soluble proteins by membrane diafiltration, Sep. Purif. Technol., 256 (2021) 117756, doi: 10.1016/j.seppur.2020.117756.
[8] S.M. Cabrera, L. Winnubst, H. Richter, I. Voigt, A. Nijmeijer, Industrial application of ceramic nanofiltration membranes for water treatment in oil sands mines, Sep. Purif. Technol. 256 (2021) 117821, doi: 10.1016/j.seppur.2020.117821.
[9] F. Elazhar, M. Elazhar, N. El Filali, S. Belhamidi, A. Elmidaoui, M. Taky, Potential of hybrid NF-RO system to enhance chloride removal and reduce membrane fouling during surface water desalination, Sep. Purif. Technol., (2021), doi: 10.1016/j.seppur.2021.118299.
[10] J. Guo, H. Bao, Y. Zhang, X. Shen, J.K. Kim, J. Ma, L. Shao, Unravelling intercalation-regulated nanoconfinement for durably ultrafast sieving graphene oxide membranes, J. Membr. Sci., 619 (2021) 118791, doi: 10.1016/j.memsci.2020.118791.
[11] S. Jamil, P. Loganathan, S.J. Khan, J.A. McDonald, J. Kandasamy, S. Vigneswaran, Enhanced nanofiltration rejection of inorganic and organic compounds from a wastewater-reclamation plant's micro-filtered water using adsorption pre-treatment, Sep. Purif. Technol., 260 (2021) 118207, doi: 10.1016/j.seppur.2020.118207.
[12] H.C. Liu, H.X. Wang, Y. Yang, Z.Y. Ye, K. Kuroda, L. Hou, *In-situ* assembly of PB/$SiO_2$ composite PVDF membrane for selective removal of trace radiocesium from aqueous environment, Sep. Purif. Technol., 254 (2021) 117557, doi: 10.1016/j.seppur.2020.117557.
[13] H. Yin, J. Zhao, Y. Li, Y. Liao, L. Huang, H. Zhang, L. Chen, Electrospun SiNPs/ZnNPs-$SiO_2$/$TiO_2$ nanofiber membrane with asymmetric wetting: ultra-efficient separation of oil-in-water and water-in-oil emulsions in multiple extreme environments, Sep. Purif. Technol., 255 (2021) 117687, doi: 10.1016/j.seppur.2020.117687.
[14] Y. Zhang, J. Guo, G. Han, Y. Bai, Q. Ge, J. Ma, C.H. Lau, L. Shao, Molecularly soldered covalent organic frameworks for ultrafast precision sieving, Sci. Adv., 7 (2021) eabe8706, doi: 10.1126/sciadv.abe8706.
[15] S. Zinadini, V. Vatanpour, A.A. Zinatizadeh, M. Rahimi, Z. Rahimi, M. Kian, Preparation and characterization of antifouling graphene oxide/polyethersulfone ultrafiltration membrane: application in MBR for dairy wastewater treatment, J. Water Process Eng., 7 (2015) 280–294.
[16] B.K. Nandi, B. Das, R. Uppaluri, M.K. Purkait, Microfiltration of mosambi juice using low-cost ceramic membrane, J. Food Eng., 95 (2009) 597–605.
[17] D. Vasanth, G. Pugazhenthi, R. Uppaluri, Fabrication and properties of low-cost ceramic microfiltration membranes for separation of oil and bacteria from its solution, J. Membr. Sci., 379 (2011) 154–163.
[18] S.A. Younssi, M. Breida, B. Achiou, Alumina membranes for desalination and Water treatment, Desal. Water Treat., (2018), doi: 10.5772/intechopen.76782.
[19] S.R. Abadi, M.R. Sebzari, M. Hemati, F. Rekabdar, T. Mohammadi, Ceramic membrane performance in microfiltration of oily wastewater, Desalination, 265 (2011) 222–228.
[20] B. Achiou, H. Elomari, A. Bouazizi, A. Karim, M. Ouammou, A. Albizane, J. Bennazha, S.A. Younssi, I.E. El Amrani, Manufacturing of tubular ceramic microfiltration membrane based on natural pozzolan for pretreatment of seawater desalination, Desalination, 419 (2017) 181–187.
[21] S. Saja, A. Bouazizi, B. Achiou, M. Ouammou, A. Albizane, J. Bennazha, S.A. Younssi, Elaboration and characterization of low-cost ceramic membrane made from natural Moroccan perlite for treatment of industrial wastewater, J. Environ. Chem. Eng., 6 (2018) 451–458.
[22] B. Ghouil, A. Harabi, F. Bouzerara, N. Brihi, Elaboration and characterization of ceramic membrane supports from raw materials used in microfiltration, Desal. Water Treat., 57 (2016) 5241–5245.
[23] H. Elomari, B. Achiou, M. Ouammou, A. Albizane, J. Bennazha, S. Alami Younssi, I. Elamrani, Elaboration and characterization of flat membrane supports from Moroccan clays. Application for the treatment of wastewater, Desal. Water Treat., 57 (2016) 20298–20306.
[24] M. Sheikhi, M. Arzani, H.R. Mahdavi, T. Mohammadi, Kaolinitic clay-based ceramic microfiltration membrane for oily wastewater treatment: assessment of coagulant addition, Ceram. Int., 45 (2019) 17826–17836.
[25] H. Aloulou, H. Bouhamed, A. Ghorbel, R. Ben Amar, S. Khemakhem, Elaboration and characterization of ceramic microfiltration membranes from natural zeolite: application to the treatment of cuttlefish effluents, Desal. Water Treat., 95 (2017) 1–9.
[26] M. Lafleur, F. Bougie, N. Guilhaume, F. Larachi, P. Fongarland, M.C. Iliuta, Development of a water-selective zeolite composite membrane by a new 404 pore-plugging technique, Microporous Mesoporous Mater., 237 (2017) 49–59.
[27] H. Aloulou, H. Bouhamed, R. Ben Amar, S. Khemakhem, New ceramic microfiltration membrane from Tunisian natural sand: application for tangential wastewater treatment, Desal. Water Treat., 78 (2017) 41–48.
[28] I. Barrouk, S.A. Younssi, A. Kabbabi, M. Persin, A. Albizane, S. Tahiri, New ceramic membranes from natural Moroccan phosphate for microfiltration application, Desal. Water Treat., 55 (2015) 53–60.
[29] A. Bouazizi, M. Breida, A. Karima, B. Achiou, M. Ouammou, J.I. Calvo, A. Aaddane, K. Khiat, S.Y. Alami, Development of a new $TiO_2$ ultrafiltration membrane on flat ceramic support made from natural bentonite and micronized phosphate and applied for dye removal, Ceram. Int., 43 (2017) 1479–1487.
[30] A. Bouazizi, S. Saja, B. Achiou, M. Ouammou, J.I. Calvo, A. Aaddane, S.A. Younssi, Elaboration and characterization of a new flat ceramic MF membrane made from natural Moroccan bentonite. Application to treatment of industrial wastewater, Appl. Clay Sci., 132–133 (2016) 33–40.
[31] M. Khemakhem, A. Oun, S. Cerneaux, M. Cretin, S. Khemakhem, R. Ben Amar, Decolorization of dyeing effluent by novel ultrafiltration ceramic membrane from low-cost natural material, J. Membr. Sci. Res., 4 (2018) 101–107.

[32] G. Singh, V.K. Bulasara, Preparation of low-cost microfiltration membranes from fly ash, Desal. Water Treat., 53 (2015) 1204–1212.
[33] K. Suresh, G. Pugazhenthi, R. Uppaluri, Fly ash based ceramic microfiltration membranes for oil-water emulsion treatment: parametric optimization using response surface methodology, J. Water Process Eng., 13 (2016) 27–43.
[34] M. Mouiya, A. Abourriche, A. Bouazizi, A. Benhammou, Y. El Hafiane, Y. Abouliatim, L. Nibou, M. Oumam, M. Ouammou, A. Smith, H. Hannache, Flat ceramic microfiltration membrane based on natural clay and Moroccan phosphate for desalination and industrial wastewater treatment, Desalination, 427 (2018) 42–50.
[35] H. Aloulou, W. Aloulou, M.O. Daramola, R. Ben Amar, Silane-grafted sand membrane for the treatment of oily wastewater via air gap membrane distillation: study of the efficiency in comparison with microfiltration and ultrafiltration ceramic membranes, Mater. Chem. Phys., 261 (2021) 124186, doi: 10.1016/j.matchemphys.2020.124186.
[36] D. Beqqour, B. Achiou, A. Bouazizi, H. Ouaddari, H. Elomari, M. Ouammou, J. Bennazha, S. Alami Younssi, Enhancement of microfiltration performances of pozzolan membrane by incorporation of micronized phosphate and its application for industrial wastewater treatment, J. Environ. Chem. Eng., 7 (2019) 102981, doi: 10.1016/j.jece.2019.102981.
[37] X. Li, Y. Mo, J. Li, W. Guo, H.H. Ngo, *In-situ* monitoring techniques for membrane fouling and local filtration characteristics in hollow fiber membrane processes: a critical review, J. Membr. Sci., 528 (2017) 187–200.
[38] R.R. Choudhury, J.M. Gohil, S. Mohanty, S.K. Nayak, Antifouling, fouling release and antimicrobial materials for surface modification of reverse osmosis and nanofiltration membranes, J. Mater. Chem. A, 6 (2018) 313–333.
[39] H. Aloulou, H. Bouhamed, M.O. Daramola, S. Khemakhem, R. Ben Amar, Fabrication of asymmetric ultrafiltration membranes from natural zeolite and their application in industrial wastewater treatment, Euro-Mediterr. J. Environ. Integr., 5 (2020) 36, doi: 10.1007/s41207-020-0150-9.
[40] W. Aloulou, W. Hamza, H. Aloulou, A. Oun, S. Khemakhem, A. Jada, S. Chakraborty, S. Curcio, R. Ben Amar, Developing of titania-smectite nanocomposites UF membrane over zeolite based ceramic support, Appl. Clay Sci., 155 (2018) 20–29.
[41] R.V. Kumar, A.K. Ghoshal, G. Pugazhenthi, Fabrication of zirconia composite membrane by in-situ hydrothermal technique and its application in separation of methyl orange, Ecotoxicol. Environ. Saf., 121 (2015) 73–79.
[42] S. Bousbih, E. Errais, F. Darragi, J. Duplay, M. Trabelsi-Ayadi, M.O. Daramola, R. Ben Amar, Treatment of textile wastewater using monolayered ultrafiltration ceramic membrane fabricated from natural kaolin clay, Environ. Technol., (2020), doi: 10.1080/09593330.2020.1729242.
[43] W. Aloulou, H. Aloulou, R. Ben Amar, Low-cost composite ultrafiltration membrane made from $TiO_2$ and nanocomposite clay materials over zeolite support for oily wastewater purification and heavy metals removal, Desal. Water Treat., 246 (2022) 166–173.
[44] S. Bousbih, R. Belhadj Ammar, R. Ben Amar, L. Dammak, F. Darragi, E. Selmane, Synthesis and evaluation of asymmetric mesoporous PTFE/clay composite membranes for textile wastewater treatment, Membranes, 11 (2021) 850, doi: 10.3390/membranes11110850.
[45] A. Manni, B. Achiou, A. Karim, A. Harrati, C. Sadik, M. Ouammou, S. Alamo Younssi, A. El Bouari, New low-cost ceramic microfiltration membrane made from natural magnesite for industrial wastewater treatment, J. Environ. Chem. Eng., 8 (2020) 103906, doi: 10.1016/j.jece.2020.103906.
[46] T. Ahmad, C. Guria, A. Mandal, Optimal synthesis and operation of low-cost polyvinyl chloride/bentonite ultrafiltration membranes for the purification of oilfield produced water, J. Membr. Sci., 564 (2018) 859–877.
[47] Y. Huang, H. Liu, Y. Wang, G. Song, L. Zhang, Industrial application of ceramic ultrafiltration membrane in cold-rolling emulsion wastewater treatment, Sep. Purif. Technol., 289 (2022) 120724, doi: 10.1016/j.seppur.2022.120724.
[48] N. Abdullah, M.A. Rahman, M.H.D. Othman, J. Jaafar, A.F. Ismail, Membranes and Membrane Processes: Fundamentals, A. Basile, S. Mozia, R. Molinari, Eds., Current Trends and Future Developments on (Bio-) Membranes: Photocatalytic Membranes and Photocatalytic Membrane Reactors, Elsevier Science, Amsterdam, 2018, pp. 45–70.
[49] M. Khemakhem, S. Khemakhem, S. Ayedi, R. Ben Amar, Study of ceramic ultrafiltration membrane support based on phosphate industry subproduct: application for the cuttlefish conditioning effluents treatment, Ceram. Int., 37 (2011) 3617–3625.
[50] R.V. Kumar, A.K. Ghoshal, G. Pugazhenthi, Elaboration of novel tubular ceramic membrane from in expensive raw materials by extrusion method and its performance in microfiltration of synthetic oily wastewater treatment, J. Membr. Sci., 490 (2015) 92–102.
[51] H. Aloulou, W. Aloulou, J. Duplay, L. Baklouti, L. Dammak, R. Ben Amar, Development of ultrafiltration kaolin membranes over sand and zeolite supports for the treatment of electroplating wastewater, Membranes, 12 (2022) 1066, doi: 10.3390/membranes12111066.
[52] G. Veréb, P. Kassai, E.N. Santos, G. Arthanareeswaran, C. Hodúr, Z. László, Intensification of the ultrafiltration of real oil-contaminated (produced) water with pre ozonation and/or with $TiO_2$, $TiO_2$/CNT nanomaterial-coated membrane surfaces, Environ. Sci. Pollut. Res., 27 (2020) 22195–22205.